SCIENTIFIC REPORTS

OPEN

SUBJECT AREAS:
SYNTHESIS AND PROCESSING
SYNTHESIS OF GRAPHENE

Received
28 October 2013

Accepted
26 March 2014

Published
11 April 2014

Correspondence and requests for materials should be addressed to S.M.W. (shumin@mail.sim.ac.cn) or Q.G. (qgong@mail.sim.ac.cn)

A novel semiconductor compatible path for nano-graphene synthesis using CBr_4 precursor and Ga catalyst

S. M. Wang[1,2], Q. Gong[1], Y. Y. Li[1], C. F. Cao[1], H. F. Zhou[1], J. Y. Yan[1], Q. B. Liu[1], L. Y. Zhang[1], G. Q. Ding[1], Z. F. Di[1] & X. M. Xie[1]

[1]State Key Laboratory of Functional Materials for Informatics, Shanghai Institute of Microsystem and Information Technology, Chinese Academy of Sciences, 865 Changning Road, Shanghai 200050, China, [2]Department of Microtechnology and Nanoscience, Chalmers University of Technology, 41296 Goteborg, Sweden.

We propose a novel semiconductor compatible path for nano-graphene synthesis using precursors containing C-Br bonding and liquid catalyst. The unique combination of CBr_4 as precursor and Ga as catalyst leads to efficient C precipitation at a synthesis temperature of 200°C or lower. The non-wetting nature of liquid Ga on tested substrates limits nano-scale graphene to form on Ga droplets and substrate surfaces at low synthesis temperatures of $T \leq 450$°C and at droplet/substrate interfaces by C diffusion via droplet edges when $T \geq 400$°C. Good quality interface nano-graphene is demonstrated and the quality can be further improved by optimization of synthesis conditions and proper selection of substrate type and orientation. The proposed method provides a scalable and transfer-free route to synthesize graphene/semiconductor heterostructures, graphene quantum dots as well as patterned graphene nano-structures at a medium temperature range of 400–700°C suitable for most important elementary and compound semiconductors.

Current research on graphene (G) has been gradually transformed from fundamental physical studies[1] toward seeking for functional device applications[2]. For graphene electronics, it is generally accepted that graphene, rather than radically taking over silicon, will complement traditional semiconductors as building blocks to replace part of the materials used in a device to enhance functionality[3]. While the problems encountered in graphene field-effect transistors (G-FETs) have been extensively investigated and solutions like use of double-layer graphene and graphene nano-ribbons (GNRs) etc. proposed and performance improved[3], attention has been paid recently toward looking into vertical transport making use of band engineering in graphene heterostructures combining graphene/semiconductors (G/S)or other 2D materials or both[4–7]. Novel device concepts like graphene barristor[6] and vertical tunneling G-FETs[7] have been proposed and current modulation in excess of 10^5 has been demonstrated. Such graphene heterostructures encompasses G/Si, G/BN and G/WS_2 etc. On the photonics side, the high intrinsic carrier mobility in graphene promises ultrafast photodetectors[8] as the intrinsic bandwidth is calculated to be >500 GHz[9]. The responsivity can be significantly increased by monolithically integrating a graphene sheet in a high finesse Fabry-Perot microcavity made of an AlGaAs/GaAs Bragg mirror[10]. The wide frequency range of optical response as a result of the gapless energy band leads to the first demonstration of graphene optical modulators operating at 1.2 GHz recently[11]. G/S heterostructures possess great flexibility in engineering electronic, transport and optical properties that are otherwise difficult or unattainable in pure graphene sheets, and may offer new technical solutions to graphene devices and potential new device concepts. Another example receiving increasing attention is graphene quantum dots (GQDs) that can emit light in a wide spectrum through size control[12]. Embedding GQDs in a semiconductor matrix could advance GQD optoelectronics like the case of semiconductor quantum dots.

To fully explore its potentials and make use of a large number of compound semiconductor family members in addition to Si and Ge, such G/S hetero- and nano-structures require monolithic (transfer-free) and semiconductor compatible synthesis techniques on large-scale substrates at low and medium temperatures (dependent on the used semiconductor material) to avoid contaminations and damages, substrate decomposition, dopant inter-diffusion and deleterious interface states. There are various methods to synthesize graphene since the first demonstration by exfoliation[13]. The exfoliated graphene has a maximum size up to mm^2 and reveals high mobility only when it is suspended[14] or transferred onto single crystal hexagonal BN[15]. Evaporation of Si atoms from SiC is

an attractive route to synthesize wafer-scale graphene but requires a very high temperature that is beyond most semiconductor substrates except Si[16–18]. Another popular method is to employ plasma enhanced or thermal chemical vapor deposition (CVD) on metal catalysts, notably Cu and Ni. However, such metal catalysts are incompatible with semiconductor processes and post-growth transfer is still required for practical applications[19–22]. Also molecular beam epitaxy (MBE) has been used as a method for graphene synthesis[23,24].Recently, a new diffusion-assisted method is reported to synthesize graphene at the Ni/substrate interface at 25–260°C by long time C diffusion through the Ni film[25]. The measured mobility is however only 667 cm^2/Vs. In summary, none of the current synthesis techniques can simultaneously meet the requirements of being monolithic, semiconductor compatible, up-scaling and grown at low-medium temperatures suitable for majority semiconductors.

In this work, we propose a new path, aiming at overcoming the above hurdles, to synthesize G/S hetero- and nano-structures at low-medium temperatures using CBr_4 combined with *in situ* prepared liquid catalysts. The tested precursor and catalysts are fully compatible with semiconductor processes. CBr_4 is a well known *p*-type dopant gas source for GaAs[26] with a maximum *p*-type doping concentration up to the range of 10^{20} cm^{-3}. We use MBE as it provides a means to ensure high carrier mobility and good interface control but the method introduced can be extended to other epitaxial or deposition techniques. Efficient cracking of CBr_4 using Ga as a catalyst on various substrates with different crystal orientations is demonstrated at temperatures down to 200°C. Nano-scale graphitization is confirmed on both Ga droplets as well as at the droplet/substrate interfaces through C diffusion. The excess Ga forms liquid droplets on substrates, which limits the graphitization size to nm scale. Some technical challenges and potential applications are discussed. The current work may open a new and potential route for making transfer-free and wafer-scale high quality G/S hetero- and nano-structures.

Results

CBr_4 as carbon precursor and Ga as liquid catalyst. We first study thermal decomposition of CBr_4 on GaAs and Ge substrates without purposely supplying Ga flux. An equivalent 2 MLs of C atoms were deposited on GaAs (001) at 400 and 690°C and on Ge (001) at 690°C, respectively. From Raman spectra, no G-peak was observed from the Ge sample while very weak G-peaks were detected from the two GaAs samples. This indicates that C precipitation through pyrolysis of CBr_4 is inefficient at these temperatures without a catalyst. CBr_4 has a melting point of 94°C and a boiling point of 190°C. It decomposes thermally via the following chemical reactions:

$$2CBr_4 \rightarrow C_2Br_6\uparrow + Br_2\uparrow$$

$$C_2Br_6 \rightarrow C_2Br_4\uparrow + Br_2\uparrow$$

The decomposition occurs already at room temperature and we do notice the sudden increase of the peak of mass number of 150 (Br_2) in mass spectrometer in the MBE chamber upon filling CBr_4 gas. C_2Br_4 has a low melting of 0°C as well as a boiling point of 244°C while C_2Br_6 also has a melting point of 160°C and a slightly high boiling point of 318°C. It should be noted that the boiling point quoted here refers to the values at atmospheric pressure. It decreases significantly in vacuum such as in an MBE chamber. The resulting Br_2 can etch GaAs or Ge forming $GaBr_3$ (melting/boiling point = 122/279°C) or $GeBr_4$, both are volatile. Therefore pure pyrolysis of CBr_4 molecules will not result in noticeable carbon precipitates on a Ge substrate and majority of the impingent molecules and consequent reactants are directly pumped away. It is well known that CBr_4 is a *p*-type dopant in GaAs with C atoms replacing As atoms and forming C-Ga bonds. The upper bound of C doping is in the 10^{20} cm^{-3} range, which contributes a weak catalytic effect and a weak G-peak in the Raman spectrum.

Based on the above discussion we then examine the Ga liquid catalytic effect using either method shown in Fig. 1. For the co-deposition method, although the Ga cell temperature was kept low, the Ga flux was still relatively higher compared with the CBr_4 flux. Unfortunately, Ga doesn't wet GaAs, Ge and Si substrates and forms droplets with a diameter of about 10–10^3 nm in both methods, but less severe in the co-deposition method. The droplet size decreases and density increases with decreasing temperature. Figure 2 shows an example for Ga droplets formed on Ge (001) at 300–320°C using both methods. The average diameter of Ga droplets is about 50 nm in

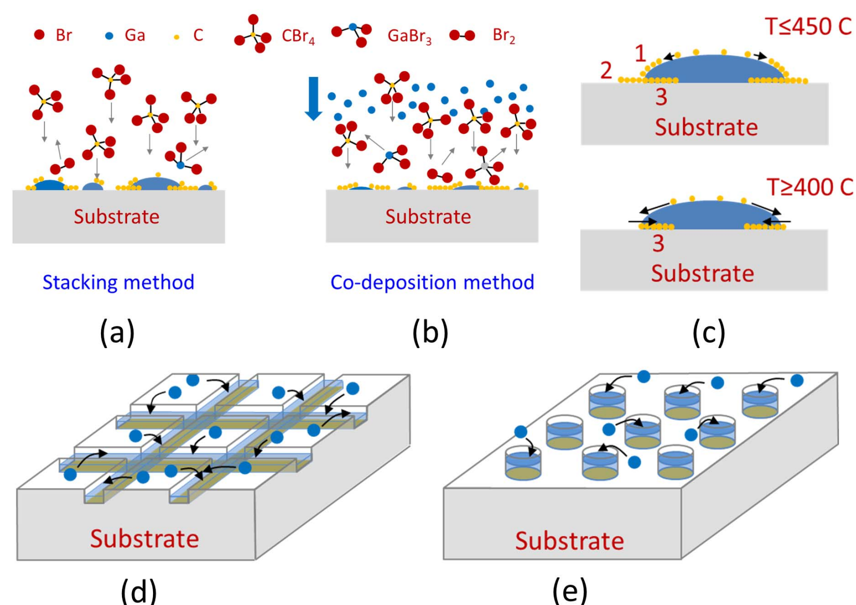

Figure 1 | Illustration of synthesis method. (a) stacking method and (b) co-deposition method, (c) shows graphene growth mode: growth on Ga top surface and substrate as marked by 1 and 2, respectively, and at the Ga-substrate interface as marked by 3, (d) and (e) show two examples of combining the current method with a shallow-etched patterned substrate for GNRs and an ordered GQD array, respectively.

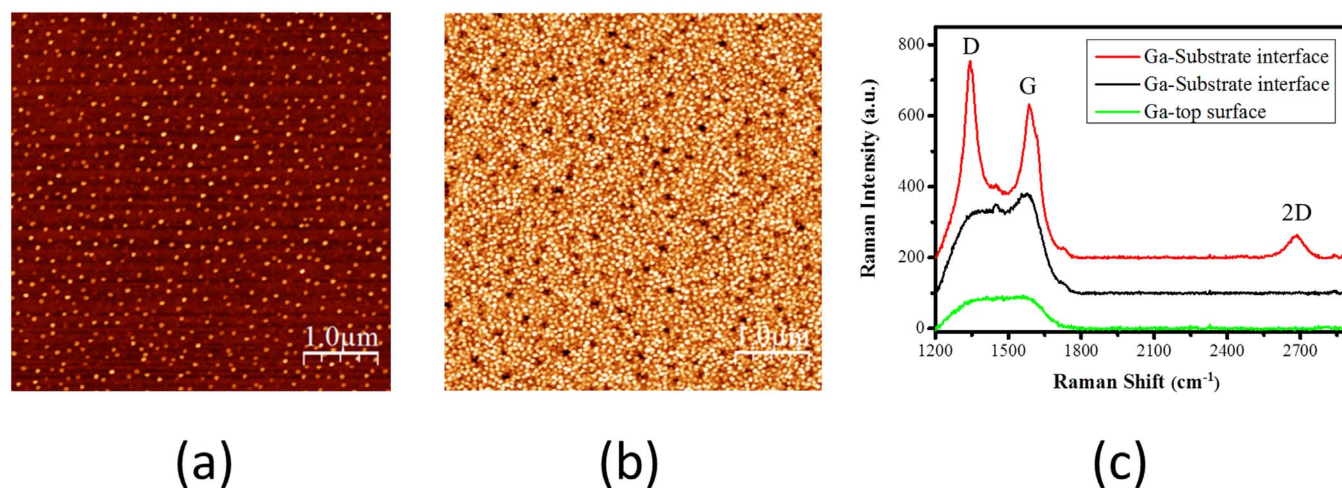

Figure 2 | AFM images (5 × 5 µm²) showing Ga droplets using the (a) co-deposition and (b) stacking method, (c) shows Raman spectra from surface and interface nano-graphene using the co-deposition method on Ge (001) at 400°C. The red curve shows Raman spectrum recorded at some spots at the Ga-substrate interface, while the black curve was recorded at other areas at the Ga-substrate interface.

both cases and the droplet density is much higher for the stacking method (2×10^{10} cm^{-2}) than for the co-deposition method (2.5×10^{9} cm^{-2}). Also the C miscibility in liquid Ga is negligible as there is no C-Ga phase diagram available. Catalytic process occurs mainly on Ga droplets and the C graphitization is formed on Ga droplets (Ga top surface, marked 1), on uncovered substrate (substrate surface, marked 2) and at droplet/substrate interfaces (Ga-substrate interface, marked 3) through C diffusion as shown in Fig. 1c. Figure 2c reveals Raman spectra from the sample synthesized at 400°C using the co-deposition method. Since the beam size in the Raman measurement is about 600 nm, much larger than the Ga droplet size, the measured signal is the sum of many nano-scale graphene. Broad and sometimes unresolved G- and D-peaks are observed which indicates that Ga acts as an effective catalyst for decomposition of CBr_4. We also transferred the sample using photo-resister and removed the Ge substrate to check the nano-graphene at the droplet/substrate interfaces. The resulting Raman signal is stronger than that on the front side as shown in Fig. 2c. In some spots, clear G-, D- and 2D-peaks are observed (the red curve in Fig. 2c), while in other area only G- and D-peaks are observed (the black curve in Fig. 2c). Raman spectroscopy is a powerful technique for assessing graphene and other crystalline or amorphous carbon. According to Ferrari, the G-peak is due to the bond stretching of sp^2 atoms in both rings and chains while the D-peak is due to the breathing modes of sp^2 atoms in rings[27]. Furthermore, he introduced criteria for classifying disorder from graphite to amorphous carbon: (1) graphite → nano-crystalline graphite; (2) nano-crystalline graphite → low sp^3 amorphous carbon and (3) low sp^3 amorphous carbon → high sp^3 amorphous carbon. We use the Lorentzian shape to simulate the merged G- and D-peaks and found the peak to be located at 1344 and 1584 cm^{-1} for the D- and G-peak, respectively. This clearly shows that the formed carbon materials fall into the first category, i.e. nano-crystalline graphene, as amorphous carbon would shift the G-peak to 1510 cm^{-1}. In addition, for the precipitated carbon at the Ga/substrate interface, a clear shoulder located at 1619 cm^{-1} is observed. This peak is a typical symptom of the nano-crystalline graphene. The size of the nano-graphene domain can be estimated to be about 5 nm using the equation of $I(D)/I(G) = C(\lambda)/L_a$, where $I(D)$ and $I(G)$ represent the intensity of the D- and G-peak, respectively, L_a the domain size and $C(\lambda) = 4.4$ nm[27]. It should be noted that such estimation only gives a low bound of the domain size. By using the integrated area ratio of the D- and G-peak and $C(\lambda) \approx 2.4 \times 10^{-10}\lambda^4$, where λ is the excitation wavelength in the Raman measurement, the estimated domain size is about 13–23 nm.

To confirm the catalytic function of liquid Ga for graphene synthesis, we employ conventional CVD in an Ar/H_2 environment using CH_4 or naphthalene as carbon sources. Large Ga droplets in mm² size were prepared by pipette on various substrates prior to being loaded into the CVD chamber. Graphene was synthesized on both surfaces of Ga droplets and at the droplet/substrate interfaces at elevated temperatures. After synthesis, the temperature was ramped down and the remained Ga droplets together with surface graphene sheets were removed. Figure 3 shows a Raman spectrum from the interface graphene using naphthalene on a GaN substrate. Uniform and pristine graphene of 1–2 monolayer thick is formed over large areas on Ga droplets and at the interfaces at a synthesis temperature of 500–700°C. This result unambiguously shows that high quality graphene is possible to be formed using liquid Ga as a catalyst on GaN at 500–700°C, a temperature range that is compatible with most important semiconductors.

We also examined the catalytic effect of other group-III elements installed in the MBE system such as Al and In. At 400°C, gallium shows a clear catalytic effect while both indium and aluminum have a negligible catalytic effect on CBr_4.

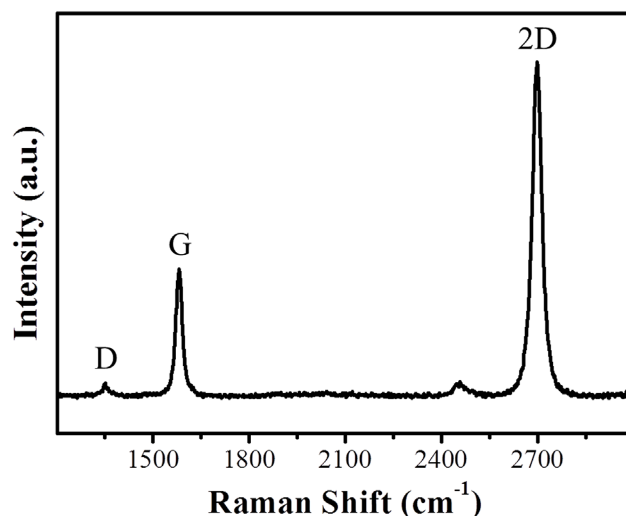

Figure 3 | Raman spectrum of pristine 1–2 monolayer interface graphene synthesized on a GaN substrate using naphthalene as C precursor and mm size liquid Ga as catalyst by CVD at 500°C.

Synthesis mode. Figure 1c shows that nano-graphene can be formed in three different regions: on Ga droplets (1), on substrate (2) and at the droplet/substrate interface (3). We call the first two cases surface mode and the last case diffusion mode. Observation of G- and D-peaks from the sample front side indicates possible nano-graphene on Ga droplets and/or substrate but we can't distinguish the two cases due to the large beam size with respect to the Ga droplet size. For this reason, we examine some large Ga droplets in μm size and perform Raman mapping. Figure 4a shows the Raman G-peak mapping from the interface of a 20 μm Ga droplet on Ge (001) using the stacking method synthesized at 1.6–11.7°C and *in situ* annealed at 720°C for 9 min. The D-peak mapping reveals a similar pattern and no 2D peak is observed. Figure 4b is the optical image from the same area for the Raman mapping. Dashed circles are guided for eye. The middle grey feature is the deformed metallic Ga. No G- and D-peaks are observed from the front side for this sample. The ring-shape nano-graphene suggests that most precipitated C atoms diffuse from the droplet edges toward center. In this sample using the stacking method, 24 ML Ga was deposited prior to CBr_4 at 1.6–11.7°C. At such low temperatures, both Ga and CBr_4 are in solid form and the 24 ML Ga will form a nm thick film in direct contact with the Ge (001) substrate. During the *in situ* annealing, Ga first melts at 29°C and form droplets since it does not wet the substrate. CBr_4 then subsequently melts and the catalytic process starts. The temperature rising time is short compared to 9 min annealing time at 720°C. Carbon diffusion can be considered to take place during the 9 min annealing. The outer edges of the Raman mapping coincide with the optical image of the droplet trace shown in Fig. 4b. This implies that graphene synthesis in the region 2 in Fig. 1c is negligible at this annealing temperature. By measuring the average width of graphene nano-ring at various annealing or synthesis temperatures and time, the activation energy for C diffusion at the Ga/Ge interface is estimated to be about 0.3 eV (see the Methods for details).

Effect of synthesis temperature and substrate. We have examined the catalytic effect of Ga on CBr_4 and quality of the resulting nano-graphene at various temperatures. A set of samples were grown using the co-deposition method on Ge (001) substrates for 200 min in the temperature range of 4–600°C. The lowest substrate temperature was 4°C and it rose during the growth up to 44°C after absorbing thermal radiation mainly from the Ge cell. So the temperature was labeled as 4–44°C below. The Ga effusion cell temperature was kept to a low value of 853°C but the incoming Ga flux (5.2×10^{12} $cm^{-2}s^{-1}$) was still higher than that of CBr_4 (3.2×10^{12} $cm^{-2}s^{-1}$). The two samples synthesized at 4–44 and 600°C were *in situ* annealed at 720–850°C for up to 120 min. Figure 5a shows Raman spectra from surface of this set of samples. Both G- and D-peaks are observed from the sample synthesized already at 200°C, again indicating the high catalytic efficiency of Ga at such a low temperature. The intensities increase with temperature, reach a maximum at 400°C and then decrease, and eventually disappear at 500°C. For samples synthesized at 500°C or higher, no Raman signals are observed from the sample surface. Instead, strong G- and D-peaks are observed from the droplet/substrate interfaces for T ≥ 400°C as shown in Fig. 5b. For the sample synthesized at 400°C, the G-peak intensity from the interface nano-grahene is about 3.7 times of that from the surface. The sample synthesized at 4–44°C and annealed at 720°C for 9 min shows further enhancement of both G- and D-peaks. These results suggest a synthesis transition from surface mode (region 1) to diffusion mode (region 3) when the synthesis temperature is above 400–450°C and the quality at the interface is in general better than that on droplets. This is understandable as C clustering on Ga droplets is a self-organized process that depends on the synthesis temperature. There is a tendency for 3D clustering instead of 2D growth at high synthesis temperatures, since CBr_4 has sp^3 hybridization. The C clustering at the droplet/substrate interfaces is restricted at the interface (C is not miscible in Ga) by 2D growth and is largely influenced by substrate type and orientation although C atoms may diffuse into the substrate.

Post-synthesis thermal annealing can further enhance G- and D-peak intensities of surface nano-graphene. Figure 5c shows an example from the sample synthesized at 450°C using the stacking method. Annealing at 800°C for 30 min enhances G- and D-peaks significantly. Annealing at even higher temperature decreases both the G- and D-peaks. The same conclusion is also confirmed from the sample synthesized at 4–44°C using the co-deposition method and subsequently annealed at 750–850°C for 30 min. (d) Comparison of Raman spectra from the samples synthesized on Si (111) and Ge (100) substrates using the co-deposition method at 400°C. The former shows higher G- and D-peaks.

We also synthesized nano-graphene on Si (111) substrates using the co-deposition method at 400°C. Figure 5d shows Raman spectra of the sample front side. The as-synthesized nano-graphene reveals 3.5 times higher intensity in the G- and D-peak compared with that grown on the Ge (001) substrate. Raman measurement from the interface nano-graphene shows, however, no increase in the G- and D-peak. This indicates that the substrate orientation plays an important role for the quality of nano-graphene although the weak van der Waals bonding between the carbon sheet and the underneath substrate is expected. The hexagonal symmetry of the Si (111) plane

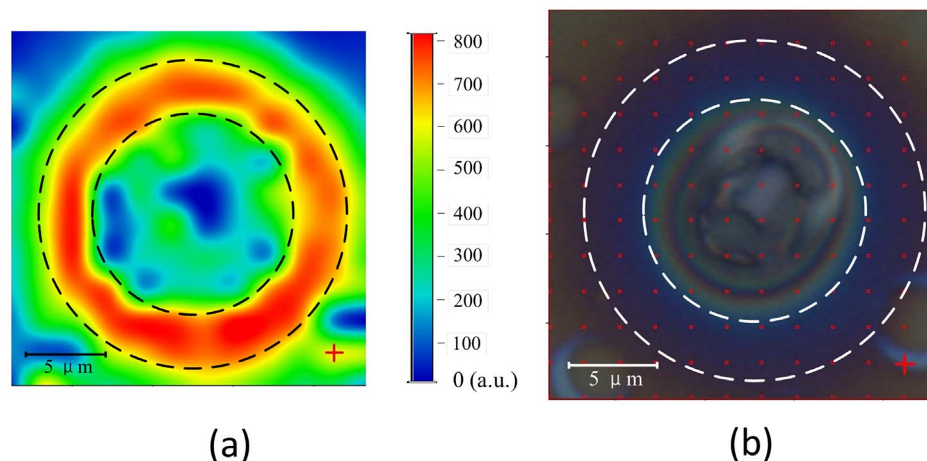

Figure 4 | (a) Raman mapping of the G-peak from a ring-shape interface nano-graphene synthesized on Ge (001) at 1.6–11.7°C and annealed at 720°C for 9 min using the stacking method, (b) shows optical image of the same area for Raman mapping. The bluish ring is the nano-graphene area with strong G- and D-peaks and the middle grey feature is deformed metallic Ga. Dashed circles are guided for eye.

Figure 5 | Raman spectra from (a) surface nano-graphene and (b) interface nano-graphene. Interface nano-graphene has higher G- and D-peaks than those of surface nano-graphene. (c) Effect of post-synthesis annealing on the Raman spectrum for the samples synthesized at 450°C using the stacking method. (d) Raman spectra from the samples synthesized on Si (111) and Ge (100) substrates using the co-deposition method at 400°C.

facilitates better ordering of precipitated C-species than on the tetragonal Ge (001) plane. The mismatch in crystal symmetry between graphene and the (001) crystal plane can induce crystal disorder and thus lower the material quality. Post-growth annealing at 1000°C for 30 min under the mixed $Ar:H_2$ (200 : 50) environment further enhances the G- and D-peak and a 2D bump is shown up. At such a temperature, Ga droplets may be partly or completely evaporated and the measured signals are the mixture of surface and interface nano-graphene. The quality is however still inferior as compared to the interface graphene on the GaN substrate synthesized at 500–700°C using CVD shown in Fig. 3. There are several possible reasons for the low quality. First, the Si substrate surface may still contain some oxides and be rough. It is not possible to grow any buffer layer before the graphene synthesis. Second, given the fact that graphene synthesized on BN reveals the best material quality[28,29], one explanation is that GaN provides stronger van der Waals bonding and thus better ordering of C atoms than Si although both have a hexagonal symmetry. Finally, the synthesis temperature of 400°C is slightly lower than that used on GN by CVD. Post-growth annealing at high temperatures can remedy some short-distance disorder but not long-distance one. Therefore the synthesis temperature is more critical than the annealing temperature for making high quality graphene.

Discussions

The mechanism for nano-graphene formation by the two synthesis methods is different. In the stacking method, C atoms precipitate on Ga droplets, whose formation has been extensively studied in droplet epitaxy[30,31]. The graphitization process occurs on surface or at the droplet/substrate interfaces via diffusion. The synthesis temperature for such a transition from surface to diffusion mode is at about 400–450°C. Repeating the alternate supply of Ga and CBr_4 increases the contact area between liquid Ga and the substrate and thus the coverage of interface graphene, but the merged large area material may contain many small domains with boundaries. This synthesis method is very attractive for making GQDs. For GQDs of interest with a size of around 10 nm, Ga droplets should be formed at room temperature and a low Ga flux is necessary. Also the low CBr_4 flux is needed to precisely control the amount of precipitated C atoms. The potential of making graphene nano-rings is attractive for exploring new phenomena in such graphene nano-structures. In the co-deposition method, the synthesis rate is determined by the CBr_4 flux and the flux ratio of CBr_4/Ga. In the Ga-rich case, excess Ga atoms will form droplets and the above scenario will occur then. If the flux ratio is properly controlled, C precipitation occurs randomly over the substrate surface. For a suitable substrate and synthesis temperature,

it should be possible to make large area G/S heterostructures using the co-deposition method.

The current work demonstrates a new class of C precursors containing halogen elements for graphene synthesis. The bonding strength of C-Br is 288 kJ/mol and is smaller than 413 kJ/mol for the C-H bond. Therefore, it is expected that CBr_4 can be catalyzed at lower temperatures than that of CH_4 which is typically around 700–1000°C using Cu and Ni as catalysts. Our results clearly show that using CBr_4 as precursor and Ga as catalyst significantly reduces the catalytic temperature. Such a combination is not limited to CBr_4 and the choice of C precursors can be of importance for ordering of C-species. In this sense, C_2Br_4, C_6Br_6 and poly-aromatic hydrocarbons are more attractive as they provide sp^2 bonding rather than sp^3 bonding in CBr_4 and C_2Br_6. This favors 2D ordering of C atoms and suppresses the 3D growth if diffusion of these small C clusters is sufficient. The formed graphene is expected to show better quality and less crystal defects. The proposed method is fully compatible with semiconductor processes and can be easily implemented in both MBE and CVD systems. One advantage of using CVD is that the precursor flux can be significantly increased and the synthesis time reduced.

The inferior quality judged by the Raman spectra is to a large extent related to the formation of non-uniform Ga droplets, substrate type and orientation. It is therefore essential to find techniques to wet Ga on selected substrates to achieve large size interface graphene. On the other hand, combination of the current method with substrate patterning prior to synthesis offers flexibility of making graphene nano-scale complexes with a desired architecture on selected areas. For example, for a patterned substrate with shallow channels or pits, the capillary effect of Ga droplets leads to liquid Ga filled in these channels and pits as shown in Fig. 1d and 1e, respectively. By engineering the size, geometry and pattern of such channels and pits, it is possible to synthesize GNRs, ordered GQDs and other nano- or micro-scale graphene complexes integrated on a semiconductor.

The synthesis temperature is very crucial. Although efficient C precipitation can be achieved at 200°C or even lower, the reactant chemicals must be efficiently evaporated to ensure a continuous catalytic process. A synthesis temperature above 400°C leads to nano-graphene formed at droplet/substrate interfaces. This is an attractive scheme for making G/S heterostructures and GQDs in a controlled way. It is interesting to note that the quality of interface graphene grown on hexagonal GaN at 500°C (Fig. 3) is superior to the counterpart grown on tetragonal Ge (001) at 600°C and on Si (111) at 400°C and further annealed at 1000°C (both are not shown), indicating that crystal symmetry and lattice mismatch between graphene and the underneath substrate play a decisive role for graphene quality. By choosing the proper substrate such as (111) plane and strong bonding, and the synthesis conditions like synthesis temperature and flux of both Ga and C precursors, it should be possible to realize high quality G/S hetero- and nano-structures using the suggested method at 400–700°C. Finally, if a surface G/S heterostructure is wanted, all the remained Ga droplets must be removed after synthesis. To make buried G/S heterostructures, the Ga droplets can be *in situ* etched or re-crystallized to form GaAs in a similar way used in the droplet epitaxy. The whole procedure can be repeated many times to form multiple G/S heterostructures or GQDs.

In conclusion, we have demonstrated a novel approach combining CBr_4 as precursors and liquid Ga catalyst to synthesize nano-scale graphene at low temperatures. The immiscible C atoms in Ga and the non-wetting nature of liquid Ga on tested substrates limit nano-scale graphene to form on Ga droplets and substrate surfaces at $T \leq 450$°C and at droplet/substrate interfaces by C diffusion via droplet edges when $T \geq 400$°C. Good quality interface nano-graphene is demonstrated and the quality can be further improved by optimization of synthesis conditions and proper selection of substrate type and orientation. The proposed method provides a viable route to fabricate graphene/semiconductor heterostructures or embed nano-scale graphene in most important elementary and compound semiconductors.

Methods

Two deposition methods, shown schematically in Fig. 1a and 1b, were employed on 2° off Ge (001), GaAs (001) and Si (111) substrates using a V90 MBE system. In the stacking method (Fig. 1a), a Ga flux was supplied for 80 seconds followed by 20 min continuous supply of 0.12 sccm CBr_4. This corresponds to a nominal C flux of 3.2×10^{12} $cm^{-2}s^{-1}$ from the calibration of C-doping in GaAs under the same CBr_4 flux. This procedure was repeated by 10 times and the sample was then annealed at 720°C for 9 min. In the co-deposition method (Fig. 1b), both Ga and CBr_4 were opened simultaneously for 200 min. The Ga cell temperature was kept low (830–860°C) and the corresponding Ga flux was in the range of $(3.7–6.9) \times 10^{12}$ $cm^{-2}s^{-1}$. The non-reacted excess Ga formed droplets on substrate surfaces. The Ge substrate was outgassed in the preparation chamber for one hour at 300°C, followed by heating up to 650°C and annealing for 20 minutes to completely remove the native oxides on the surface. For the Si substrate, the substrate was thermally cleaned at 720°C for 5 minutes in the growth chamber. The GaAs substrate was heated up to 675°C and annealed for 10 minutes under the arsenic flux for thermal desorption of native oxides, followed by deposition of a 200 nm thick GaAs buffer to smoothen the surface. The synthesis temperature was measured between 4 to 600°C by the thermocouple. For some samples, post-growth thermal annealing was performed at 750–1000°C for up to 120 min.

In order to measure the interface graphene, the transferring of the graphene deposited on a germanium substrate was carried out. A layer of poly (methyl methacrylate) (PMMA) was spin coated on the substrate prior to the transfer. Afterwards the detachment of the PMMA/graphene layer from the initial surface was done by etching the germanium substrate with a solution ($HF:HNO_3:H_2O = 1:1:2$) at room temperature. After the substrate was completely removed, the PMMA/graphene membrane was obtained and moved from solution to DI water. Finally, the membrane was flipped over in water and laid over the target substrate with the graphene layer facing up.

The activation energy for C diffusion at the Ga/Ge interface, E, was estimated from the measured diffusion length, L, which can be expressed by $L = \sqrt{D_0 \exp(-E/kT)\tau}$, Where D_0 is a constant, k is Boltzmann constant, T is synthesis temperature in Kelvin and τ is synthesis time. All the L, T and τ are measureable or known parameters for each sample. The activation energy was estimated from the slope by plotting $\ln(L^2/D_0)$ versus $1/kT$.

1. Castro Neto, A. H. & Novoselov, K. New directions in science and technology: two-dimensional crystals. *Rep. Prog. Phys.* **74**, 082501 (2011).
2. Novoselov, K. S. *et al.* A roadmap for graphene. *Nature* **490**, 192–200 (2012).
3. Schwierz, F. Graphene transistors: status, prospects, and problems. *Proc. IEEE* **101**, 1567–1584 (2013).
4. Britnell, L. *et al.* Field-Effect tunneling transistor based on vertical graphene heterostructures. *Science* **335**, 947–950 (2011).
5. Mehr, W. *et al.* Vertical graphene base transistor. *IEEE Electron. Dev. Lett.* **33**, 691–693 (2012).
6. Yang, H. *et al.* Graphene barristor, a triode device with a gate-controlled Schottky barrier. *Science* **336**, 1140–1143 (2012).
7. Georgiou, T. *et al.* Vertical field-effect transistor based on graphene–WS_2 heterostructures for flexible and transparent electronics. *Nat. Nanotechnol.* **8**, 100–103 (2013).
8. Mueller, T., Xia, F. & Avouris, P. Graphene photodetectors for high-speed optical communications. *Nat. Photonics* **4**, 297–301 (2010).
9. Xia, F., Mueller, T., Lin, Y., Valdes-Garcia, A. & Avouris, P. Ultrafast graphene photodetector. *Nat. Nanotechnol.* **4**, 839–843 (2009).
10. Furchi, M. *et al.* Microcavity-Integrated Graphene Photodetector. *Nano Lett.* **12**, 2773–2777 (2012).
11. Liu, M. *et al.* A graphene-based broadband optical modulator. *Nature* **474**, 64–67 (2011).
12. Peng, J. *et al.* Graphene quantum dots derived from Carbon fibers. *Nano Lett.* **12**, 844–849 (2012).
13. Novoselov, K. S. *et al.* Electric field effect in atomically thin carbon films. *Science* **306**, 666–669 (2004).
14. Bolotin, K. I. *et al.* Ultrahigh electron mobility in suspended graphene. *Solid State Commun.* **146**, 351–355 (2008).
15. Dean, C. R. *et al.* Boron nitride substrates for high-quality graphene electronics. *Nat. Nanotechnol.* **5**, 722–726 (2010).
16. Rollings, E. *et al.* Synthesis and characterization of atomically thin graphite films on a silicon carbide substrate. *J. Phys. Chem. Solids* **67**, 2172–2177 (2006).
17. Juang, Z. Y. *et al.* Synthesis of graphene on silicon carbide substrates at low temperature. *Carbon* **47**, 2026–2031 (2009).
18. Tedesco, J. L. *et al.* Hall effect mobility of epitaxial graphene grown on silicon carbide. *Appl. Phys. Lett.* **95**, 122102 (2009).
19. Sun, Z. *et al.* Growth of graphene from solid carbon sources. *Nature* **468**, 549–552 (2010).

20. Li, X. S. *et al.* Large-area synthesis of high-quality and uniform graphene films on copper foils. *Science* **324**, 1312–1314 (2009).
21. Bae, S. *et al.* Roll-to-roll production of 30-inch graphene films for transparent electrodes. *Nat. Nanotechnol.* **5**, 574–578 (2010).
22. Su, C. Y. *et al.* Direct Formation of wafer scale graphene thin layers on insulating substrates by chemical vapor deposition. *Nano Lett.* **11**, 3612–3616 (2011).
23. Jerng, S. K. *et al.* Nanocrystalline graphite growth on sapphire by carbon molecular beam epitaxy. *J. Phys. Chem. C* **115**, 4491–4494 (2011).
24. Moreau, E. *et al.* Graphene growth by molecular beam epitaxy on the carbon-face of SiC. *Appl. Phys. Lett.* **97**, 241907 (2010).
25. Kwak, J. *et al.* Near room-temperature synthesis of transfer-free graphene films. *Nat. Commun.* **3**, 645 (2012).
26. Malik, R. J., Nottenberg, R. N., Schubert, E. F., Walker, J. F. & Ryan, R. W. Carbon doping in molecular beam epitaxy of GaAs from a heated graphite filament. *Appl. Phys. Lett.* **53**, 2661–2663 (1988).
27. Ferrari, A. C. Raman spectroscopy of graphene and graphite: Disorder, electron–phonon coupling, doping and nonadiabatic effects. *Solid State Commun.* **143**, 47–57 (2007)
28. Yang, W. *et al.* Epitaxial growth of single-domain graphene on hexagonal boron nitride. *Nat. Mat.* **12**, 792–797(2013).
29. Usachov, D. *et al.* Quasi freestanding single-layer hexagonal boron nitride as a substrate for graphene synthesis. *Phys. Rev. B* **82**, 075415 (2010).
30. Koguchi, N. *et al.* New MBE growth method for InSb quantum well boxes. *J. Crystal Growth* **111**, 688–692 (1991).
31. Watanabe, K. *et al.* Fabrication of GaAs quantum dots by modified droplet epitaxy. *Jpn. J. Appl. Phys.* **39**, 79–81 (2000).

Acknowledgments

This work was supported in part by Chinese Academy of Sciences, and carried out at the State Key Laboratory of Functional Materials for Informatics, supported by the National Natural Science Foundation of China (Grant No. 61321492), the Key Research Program of the CAS (Grant No. KGZD-EW-804), and CAS international collaboration and innovation program on high mobility materials engineering.

Author contributions

S.M.W. conceived the original idea, guided the project and wrote the manuscript. Q.G. and Q.B.L. developed and performed graphene synthesis by MBE. Y.Y.L., C.F.C., H.F.Z., J.Y.Y. and L.Y.Z. carried out material characterization. G.Q.D. performed graphene synthesis by CVD. Z.F.D. and X.M.X. contributed to project planning. All authors assisted with the manuscript preparation and discussed the results.

Additional information

Competing financial interests: The authors declare no competing financial interests.

How to cite this article: Wang, S.M. *et al.* A novel semiconductor compatible path for nano-graphene synthesis using CBr_4 precursor and Ga catalyst. *Sci. Rep.* **4**, 4653; DOI:10.1038/srep04653 (2014).

This work is licensed under a Creative Commons Attribution-NonCommercial-ShareAlike 3.0 Unported License. The images in this article are included in the article's Creative Commons license, unless indicated otherwise in the image credit; if the image is not included under the Creative Commons license, users will need to obtain permission from the license holder in order to reproduce the image. To view a copy of this license, visit http://creativecommons.org/licenses/by-nc-sa/3.0/